Available online at www.sciencedirect.com

SciVerse ScienceDirect

Ceramics International 38 (2012) 2461–2466

CERAMICS INTERNATIONAL

www.elsevier.com/locate/ceramint

Effect of substrate temperature on the properties of TiO_2 nanoceramic films

Su-Shia Lin *

Department of Applied Materials and Optoelectronic Engineering, National Chi Nan University, Puli, Nantou Hsien 54561, Taiwan, ROC

Received 14 August 2011; received in revised form 4 November 2011; accepted 4 November 2011
Available online 10 November 2011

Abstract

TiO_2 nanoceramic films were deposited on glasses by rf magnetron sputtering. This method provides more advantages in controlling the microstructure and composition of the films. TiO preferentially formed and the deposited films tended to become nonstoichiometric by increasing substrate temperature. The morphologies and hydrophilic properties of TiO_2 films were significantly affected by the substrate temperature. The nonlinear refractive index of the TiO_2 film on the glass substrate measured by Moiré deflectometry was of the order of 10^{-8} cm^2 W^{-1}. Smaller grain size, higher optical energy gap, visible transmission and linear refractive index, and lower stress-optical coefficient were obtained at lower substrate temperature.

Keywords: Film; Sputtering; Substrate temperature; Transmission; Refractive index

1. Introduction

There has been increasing interest in the fabrication of TiO_2 thin films because they present useful optical, electrical, and chemical properties such as high refractive index [1], high relative dielectric constant [2], remarkable solar energy conversion [3,4], and photocatalysis [5]. Therefore, TiO_2 thin film can be a promising material for an optical filter [6], antireflection film [7], a self-cleaning coating [8], a high efficient dielectric [9], and a solar cell [10]. TiO_2 thin films have been prepared by several techniques, including chemical vapor deposition [11], aerosol pyrolysis [12], electrodeposition [13], sol–gel process [14], evaporation [15] and various sputtering methods [16,17].

Among these techniques, rf magnetron sputtering method provides more advantages in controlling the microstructure and composition of the films [18]. The characteristics of films are affected by the preparation conditions such as working pressure, substrate temperature, types of substrates, and the thickness of the films [19]. In this study, TiO_2 nanoceramic films were prepared by rf magnetron sputtering. The effect of substrate temperature on the properties of TiO_2 nanoceramic films was investigated.

Transparent materials generally exhibit the optical Kerr effect. The nonlinear refractive indices of materials are of great interest because of potential applications in designing optical devices and laser technology [20–23]. Moiré deflectometry is a powerful tool for measuring the nonlinear refractive indices of materials. The main advantages of the Moiré deflectometry technique are its extreme experimental simplicity, lower cost and lower sensitivity to external disturbances than other interferometric methods. In this study, this method is applied to measure the nonlinear refractive indices of TiO_2 films on glass substrates under illumination with a 5-mW He–Ne laser (λ = 632.8 nm).

2. Experimental procedures

The TiO_2 nanoceramic films were deposited on glass (Corning 1737) by rf magnetron sputtering. The target used in this study was sintered stoichiometric TiO_2 (99.99% purity, 5 cm diameter, 5 mm thickness, Target Materials Inc., USA). The dimension of the glass substrates was 24 mm × 24 mm × 1.1 mm. Before deposition, the substrates were ultrasonically cleaned in alcohol, rinsed in deionized water and dried in nitrogen. The sputtering was performed in an Ar atmosphere with a target-to-substrate distance of 15 cm. A turbo-molecular pump backed by a rotary pump, was used to achieve a base pressure of 1.3×10^{-4} Pa. For the deposition of

* Tel.: +886 49 2910960x4771; fax: +886 49 2912238.
E-mail address: sushia@ncnu.edu.tw.

0272-8842/$36.00
doi:10.1016/j.ceramint.2011.11.014

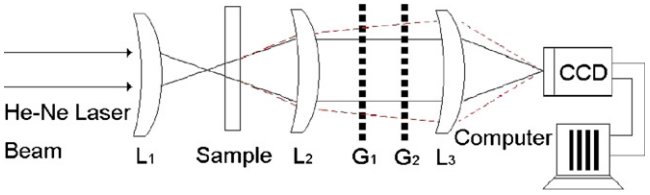

Fig. 1. The experimental set-up for measuring index of nonlinear refraction by Moiré deflectometry technique.

the films, the substrate temperature was controlled in the range of 100–500 °C. The working pressure was 1.5 Pa. No external bias voltage was applied to the substrate. An rf power (13.56 MHz, RGN-1302, ULVAC, Japan) of 50 W was supplied to the TiO_2 target. The rotating speed of the substrate was 20 rpm, and the thickness of films was maintained at 100 nm.

The film thickness was measured using a surface profiler (Alpha-Step 500, TENCOR, Santa Clara, CA). The elemental compositions were investigated by X-ray photoemission spectroscopy (XPS; PHI 5000 VersaProbe, Japan). X-ray diffraction (XRD; Rigaku D/MAX2500, Japan) was used to study the crystal structure. The surface morphologies and surface roughness were examined by atomic force microscopy (AFM; Digital Instruments Inc., NanoScope E, USA). The water contact angles on films were measured by contact angle meter (Model 100SB, Sindatek, Taiwan). The optical transmission spectra of films in the ultraviolet–visible–infrared (UV–vis–IR) region were obtained using a spectrophotometer (HP 8452A Diode Array Spectrophotometer, Hewlett Packard, Palo Alto, CA). The linear refractive indices of films were recorded using a spectrometer (MP100-ST, Fremont, CA). The stress was measured by Nano Indenter XP System (MTS Systems Corporation, MN, USA).

Fig. 1 shows the Moiré deflectometry experimental set-up that is used to measure the nonlinear refractive indices of TiO_2 films on glass substrates. A 5-mW He–Ne laser beam (wavelength of 632.8 nm) was focused by lens L_1 and is re-collimated by lens L_2. The focal lengths of lenses L_1, L_2 and L_3 were all −250 mm. Two similar Ranchi gratings G_1 and G_2 with a pitch of 0.1 mm were used to construct the Moiré fringe patterns. The distance between the planes of G_1 and G_2 was set to 64 mm, which is one of the Talbot distances of the used gratings. The Talbot distances satisfy $z_t = tp^2/\lambda$ where p is the periodicity of the grating; λ is the wavelength of light, and t is an integer. In this work, the Moiré fringes were clearly formed at a Talbot distance of $z_{t=4} \approx 64$ mm. The Moiré fringe patterns were projected onto a computerized CCD camera by lens L_3, which was placed at the back of the second grating.

3. Results and discussion

3.1. Film composition

Fig. 2 shows the X-ray diffraction patterns of TiO_2 films prepared at various substrate temperatures. XRD analysis was conducted on the films using a Rigaku D/MAX2500 goniometer with 18 kW rotating anode X-ray, equipped with a thin film attachment unit. The equipment was operated with Cu Kα (λ = 1.5418 Å) radiation at 40 kV, 100 mA and a scanning speed of 4° min^{-1} at an incident angle of 3°. The interval of the scan was 0.01° and the scanning range was 10–80°. In Fig. 2, the nanocrystalline anatase TiO_2 film was observed at the substrate temperature of 300 °C. However, when the substrate temperature was increased to 400 °C, the coexistence of nanocrystalline TiO_2 and TiO was observed.

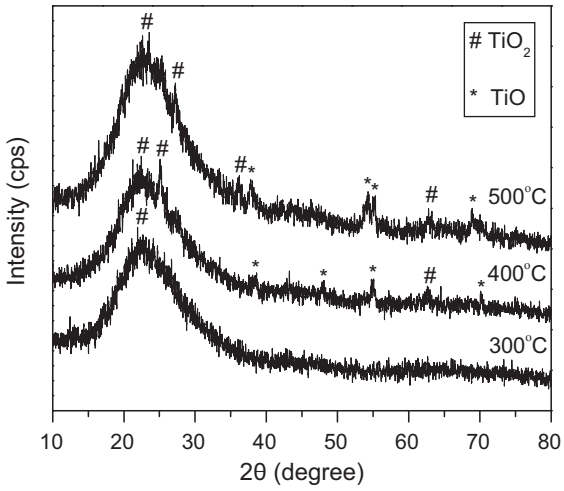

Fig. 2. The X-ray diffraction patterns of TiO_2 films prepared at various substrate temperatures.

The highest and the lowest energy components have been assigned to Ti^{4+} and Ti^0, respectively, while the intermediate component has the energy shift relative to TiO_2 that falls in between that of Ti^{3+} and Ti^{2+} [24]. Radecka [24] and Zakrzewska [25] studied TiO_2 thin films and reported that one can expect at least Ti^{3+} and Ti^{2+} oxidation states as a result of the deviation from stoichiometry, besides Ti^{4+} related to TiO_2. The substantial contributions from lower oxidation states (Ti^{3+} or Ti^{2+} and Ti^0) have been observed at the largest oxygen deficiency. According to Fig. 2, TiO formed preferentially when the substrate temperature increased. It suggested that the deposited films became nonstoichiometric by increasing substrate temperature.

Table 1 shows the elemental composition of TiO_2 films deposited at various substrate temperatures. The Ti content of the sputtered films increased with the substrate temperature. The O/Ti atomic ratio decreased with increasing the substrate temperature. This suggested that the deposited films became nonstoichiometric by increasing the substrate temperature. This was in agreement with the results of Fig. 2.

Table 1
Elemental composition of the TiO_2 films, deposited at various substrate temperatures, obtained by XPS.

Substrate temperature (°C)	O content (at.%)	Ti content (at.%)	O/Ti
100	59.9	40.1	1.49
200	59.5	40.5	1.47
300	59.1	40.9	1.44
400	58.3	41.7	1.40
500	57.8	42.2	1.37

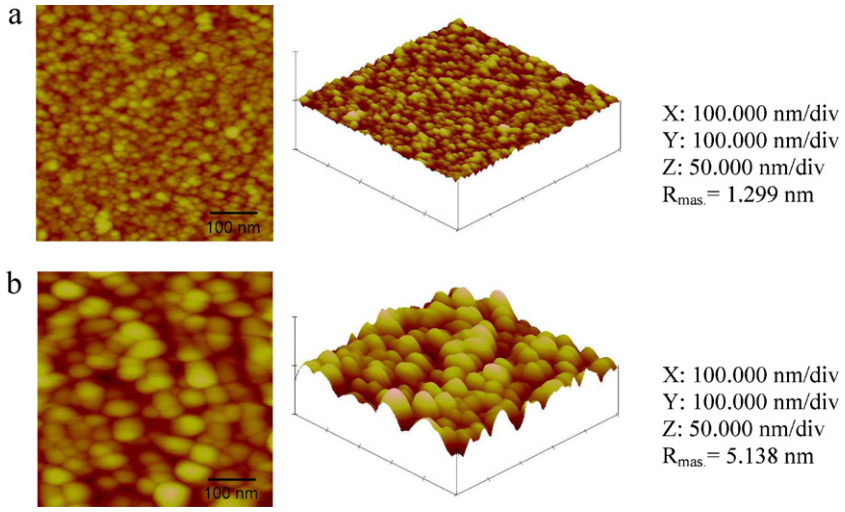

Fig. 3. The morphologies of TiO_2 prepared at (a) 100 °C and (b) 500 °C.

Fig. 3 shows the morphologies of TiO_2 films prepared at (a) 100 °C and (b) 500 °C. In Fig. 3a, TiO_2 films were composed of irregular grains with grain size of 15–35 nm and only a few pores. According to Fig. 3a and b, the average grain size, porosity and root-mean-square (RMS) roughness increased with substrate temperature. The TiO_2 films prepared at 500 °C, the kinetic energies of particles were high. It is likely that the particles arrived at the substrate with high kinetic energy, and high rate led to high porosity and high roughness [26].

Fig. 4 shows water contact angles on TiO_2 films deposited at various substrate temperatures. Wettability of a solid surface with liquids is not only governed by its chemical properties but also by its geometry. Hydrophilic property is well known to be enhanced by fine roughness [1]. Therefore, a control of surface microstructure of the films is a way to improve the hydrophilic properties. The hydrophilic properties of TiO_2 films were evaluated by examining the water contact angle on TiO_2 films. The water contact angle decreased with the increase of substrate temperature. It suggested that the hydrophilic properties of TiO_2 films were improved by increasing substrate temperature.

3.2. Optical properties

The optical energy gap E_g could be obtained from the intercept of $(\alpha h\nu)^2$ versus $h\nu$ for direct allowed transitions [27]. Better linearity was observed for $(\alpha h\nu)^2$ versus $h\nu$ [27,28] as shown in Fig. 5. The E_g decreased with the increase of substrate temperature and to be a value of 3.7 eV at 500 °C. The change of optical energy gap E_g after increasing substrate temperature has been interpreted as a Moss–Burstein shift, where the change is the result of a large decrease in the free carrier concentration, and the corresponding downward shift of the Fermi level to below the band edge [29,30].

Fig. 6 shows the transmission in the UV–vis–IR region of TiO_2 films prepared at various substrate temperatures. It could be observed that the transmission in the visible region decreased substantially at short wavelengths near the ultraviolet

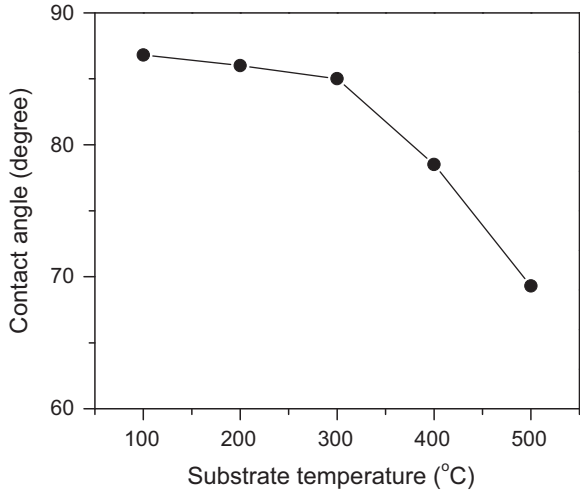

Fig. 4. Water contact angles on TiO_2 films deposited at various substrate temperatures.

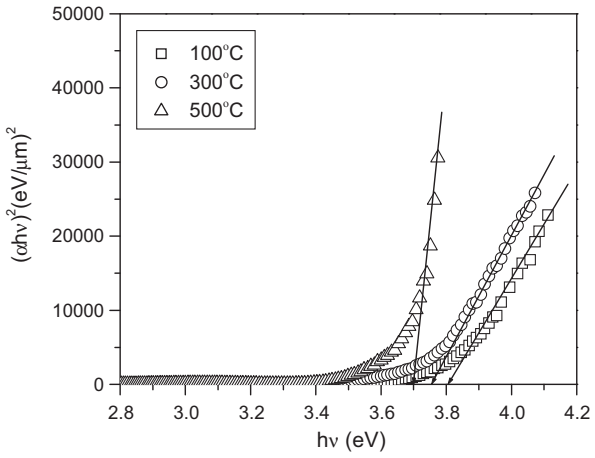

Fig. 5. Plots of $(\alpha h\nu)^2$ versus $h\nu$ for TiO_2 films prepared at various substrate temperatures.

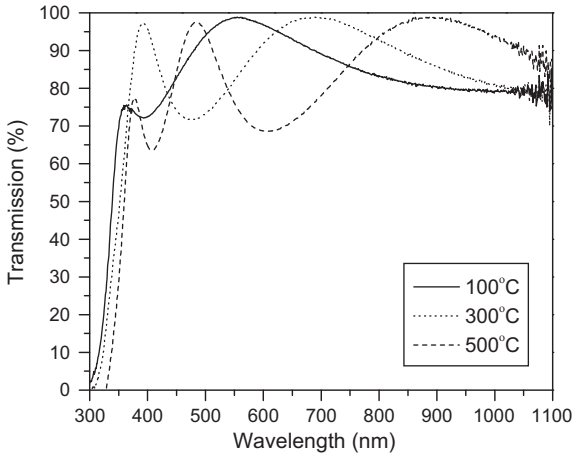

Fig. 6. The transmission in the UV–vis–IR region of TiO_2 films prepared at various substrate temperatures.

range for all films. By comparison, the absorption edge was observed at a slightly lower wavelength range for films prepared at lower substrate temperature. The shift of absorption edge may be attributed to the difference in grain size [31–33]. From the previous discussion of AFM images (Fig. 3), the TiO_2 film prepared at lower substrate temperature contained relatively small grain size. It corresponded to the blue shift of absorption edge. Similar results were reported by Yu et al. [31], Li et al. [32] and Lin et al. [33].

The average visible transmission of TiO_2 films prepared at various substrate temperatures was shown in Fig. 7. According to Figs. 5 and 7, the TiO_2 film had higher optical energy gap and exhibited higher average visible transmission at lower substrate temperature. It was probably due to the relatively low surface roughness, which could result in less light scattering [34]. It was also probably due to the reduced porosity, which absorbed less light [35]. These results indicated that the substrate temperature affected the transmission of films significantly.

The index of refraction, n, which depends on the radiation intensity, may be expressed in terms of the nonlinear index

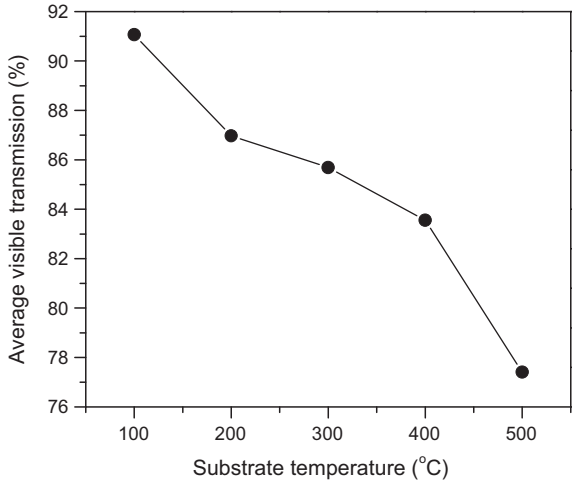

Fig. 7. The average visible transmission of TiO_2 films prepared at various substrate temperatures.

n_2 ($cm^2\ W^{-1}$):

$$n(r,z) = n_o + n_2 I(r,z) = n_o + \Delta n(r,z) \tag{1}$$

where n_o is the linear index of refraction, $I(r, z)$ is the irradiance of the laser beam within the sample, and $\Delta n(r, z)$ is the light-induced change in refractive index. Based on the assumption that a Gaussian beam is traveling in the $+z$ direction, the beam irradiance can be written as

$$I(r,z) = I_0 \frac{\omega_0^2}{\omega^2(z)} \exp\left[-\frac{2r^2}{\omega^2(z)}\right] \tag{2}$$

where r is the radial radius of the imaginary sphere; ω_0 is the spot size of the beam at the focus; $\omega(z) = \omega_0(1 + z^2/z_0^2)^{1/2}$ is the beam radius at a distance z from the position of the waist; $z_0 = \pi\omega_0^2/\lambda$ is the diffraction length of the Gaussian beam, and λ is the wavelength. The irradiance of the beam at the focus is denoted I_0 and in terms of the input laser power, p_{in}, equals $2p_{in}/\pi\omega_0^2$. Therefore, for a Gaussian laser beam, the radial dependence of the irradiance gives rise to a radially dependent parabolic refractive index change near the beam axis:

$$\Delta n(r,z) = n_2 I_0 \frac{\omega_0^2}{\omega^2(z)} \exp\left[-\frac{2r^2}{\omega^2(z)}\right] \tag{3}$$

Moiré deflectometry is a sensitive technique for measuring changes in the refractive indices of materials. The sensitivity of this technique is determined by the minimum measurable-angle of rotation (α_{min}). The tested sample was placed at various distances from the focal point of lens L_1, and the minimum angle of rotation was obtained. The same experiment was performed by using only a pure glass substrate to check the contribution of the glass substrate to the nonlinear refraction measurement. No observed fringe rotation or change in fringe size was found.

For the thin nonlinear medium of thickness d, the lowest nonlinear refractive index can be written as

$$n_{2,min} = \frac{\theta f_2^2}{z_t} \frac{\pi\omega_0^4}{d\, p_{in} z_0^2} \alpha_{min} \tag{4}$$

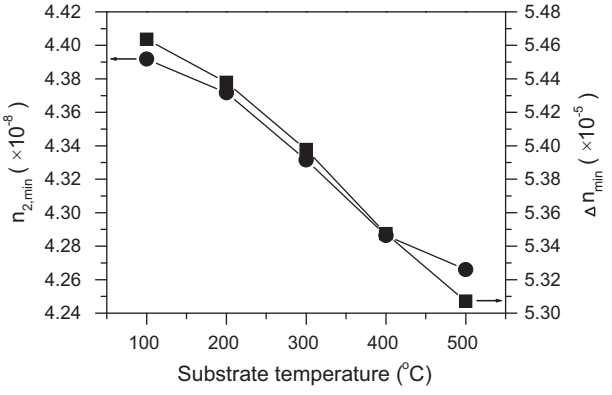

Fig. 8. The minimum nonlinear refractive indices and the change in the minimum refractive indices of TiO_2 films prepared at various substrate temperatures on glass substrates.

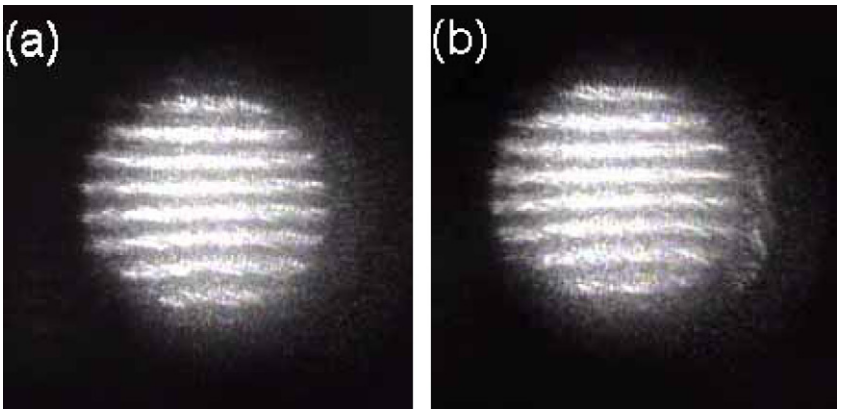

Fig. 9. The Moiré fringe patterns of TiO_2 prepared at (a) 100 °C and (b) 500 °C.

and the change in the minimum refractive index is

$$\Delta n_{\min} = \frac{\omega_0^2 \theta f_2^2}{2dz_t z_0^2} \alpha_{\min} \quad (5)$$

Fig. 8 shows the minimum nonlinear refractive indices and the change in the minimum refractive indices of TiO_2 films prepared at various substrate temperatures on glass substrates. The nonlinear refraction index was measured to be of the order of 10^{-8} cm^2 W^{-1} and the change in refractive index was of the order of 10^{-5}.

Fig. 9 shows the Moiré fringe patterns of TiO_2 films prepared at (a) 100 °C and (b) 500 °C By comparing Fig. 9a with Fig. 9b, the changes in sizes of the Moiré fringes were observed. It was probably due to the more pores in TiO_2 films prepared at 500 °C.

A change of the linear refractive index caused by stress is called the photoelastic effect [36]. The linear refractive index is specified by the indicatrix, which is an ellipsoid whose coefficients are the components of the relative dielectric impermeability tensor B_{ij} at optical frequencies:

$$B_{ij} x_i x_j = 1 \quad (6)$$

The small change of the linear refractive index produced by stress is a small change in the shape, size and orientation of the indicatrix. This change is specified by the small changes in the coefficients B_{ij}.

If terms of higher order than the first in the field of stresses are neglected, then the changes ΔB_{ij} in the coefficients are

$$\Delta B_{ij} = \varphi_{ijkl} \sigma_{kl} \quad \text{or} \quad \Delta B_{ij} = p_{ijrs} \varepsilon_{rs} \quad (7)$$

where φ_{ijkl} and p_{ijrs} are called the piezo-optical and strain-optical coefficients, which typically have the orders of magnitude of 10^{-12} Pa^{-1} and 10^{-1} Pa^{-1}, respectively.

Based on the relation, $B = 1/n_0^2$, the change of linear refractive index for an isotropic film material is assumed to be [36,37]

$$\left(\frac{\partial n_0}{\partial \sigma}\right)_T = -\frac{1}{2} n_0^3 \varphi \quad (8)$$

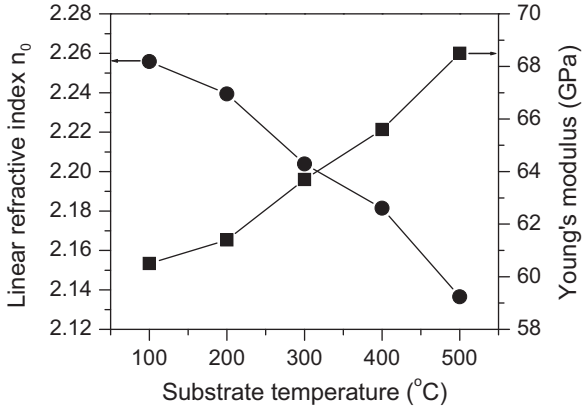

Fig. 10. The linear refractive indices and Young's moduli of TiO_2 films prepared at various substrate temperatures.

Consequently, a change in the linear refractive index due to film stress may affect the optical performance of an optical thin film, as shown in Eq. (8).

Fig. 10 shows the linear refractive indices and Young's moduli of TiO_2 films prepared at various substrate temperatures. The linear refractive index n_0 was measured at a wavelength of 632.8 nm. The linear refractive index of TiO_2 film decreased with the substrate temperature. However, the stress of TiO_2 film increased with the substrate temperature. The linear refractive index was found to correlate with the porosity [38,39]. It indicated that a dense TiO_2 film with a high linear refractive index and low stress could be obtained by decreasing substrate temperature.

The value of $\Delta n/\Delta \sigma$ is reportedly similar to the stress-optical coefficient [40]. The stress-optical coefficient, $(\partial n_0/\partial \sigma)_T$, of a TiO_2 film was evaluated and was in the range of -1.85×10^{-12} to -14.5×10^{-12} Pa^{-1}. Lower porosity corresponds to a lower stress-optical coefficient for the same material [39].

4. Conclusions

The nanocrystalline anatase of TiO_2 film preferentially formed when the substrate temperature was decreased. The

porosity, surface roughness and hydrophilic property increased with the substrate temperature. The nonlinear refraction index of the TiO_2 film on the glass substrate was measured to be of the order of 10^{-8} cm^2 W^{-1} and the change in the refractive index was of the order of 10^{-5}. The visible transmission of TiO_2 film increased by decreasing substrate temperature. Higher optical energy gap and linear refractive index, and lower stress-optical coefficient were obtained at lower substrate temperature.

Acknowledgement

The author would like to thank the National Science Council of the Republic of China, Taiwan, for financially supporting this research under Contract No. NSC-100-2221-E-260-014.

References

[1] A.S. Guzenda, M.G. Lipman, H. Szymanowski, J. Kowalski, P. Wojciechowski, T. Halamus, A. Tracz, Characterization of thin TiO_2 films prepared by plasma enhanced chemical vapour deposition for optical and photocatalytic applications, Thin Solid Films 517 (2009) 5409–5414.
[2] M. Okada, Y. Yamada, P. Jin, M. Tazawa, K. Yoshimura, Fabrication of multifunctional coating which combines low-e property and visible-light-responsive photocatalytic activity, Thin Solid Films 442 (2003) 217–221.
[3] B. O'Regan, M. Gratzel, A low-cost, high-efficiency solar cell based on dye-sensitized colloidal TiO_2 films, Nature 353 (1991) 737–740.
[4] M.K Nazeeruddin, A. Kay, I. Rodicio, R. Humphry-Baker, E. Muller, P. Liska, N. Vlachopoulos, M. Gratzel, Conversion of light to electricity by cis-X2bis(2,2′-bipyridyl-4,4′-dicarboxylate)ruthenium(II) charge-transfer sensitizers (X = Cl–, Br–, I–, CN–, and SCN–) on nanocrystalline titanium dioxide electrodes, J. Am. Chem. Soc. 115 (1993) 6382–6390.
[5] S. Takeda, S. Suzuki, H. Odaka, H. Hosono, Photocatalytic TiO_2 thin film deposited onto glass by DC magnetron sputtering, Thin Solid Films 392 (2001) 338–344.
[6] S. Laurouche, H. Szymanowski, J.E. Klemberg-Sapieha, L. Martinu, Microstructure of plasma-deposited SiO_2/TiO_2 optical films, J. Vac. Sci. Technol. A 22 (2004) 1200–1207.
[7] K. Yeng, Y. Lam, A simple chemical vapour deposition method for depositing thin TiO_2 films, Thin Solid Films 109 (1983) 169–178.
[8] J.C. Yu, J. Yu, W. Ho, J. Zhao, Light-induced super-hydrophilicity and photocatalytic activity of mesoporous TiO_2 thin films, J. Photochem. Photobiol. A: Chem. 148 (2002) 331–339.
[9] C.J. Taylor, D.C. Gilmer, D.G. Colombo, G.D. Wilk, S.A. Campbell, J. Robert, W.L. Gladfelter, Does chemistry really matter in the chemical vapor deposition of titanium dioxide? Precursor and kinetic effects on the microstructure of polycrystalline films, J. Am. Chem. Soc. 121 (1991) 5220–5229.
[10] Y. Saito, S. Kambe, T. Kitamura, Y. Wada, S. Yanagida, Morphology control of mesoporous TiO_2 nanocrystalline films for performance of dye-sensitized solar cells, Sol. Energy Mater. Sol. Cells 83 (2004) 1–13.
[11] Y. Guo, X.W. Zhang, G.R. Han, Investigation of structure and properties of N-doped TiO_2 thin films grown by APCVD, Mater. Sci. Eng. B 135 (2006) 83–87.
[12] L. Kavan, M. Grätzel, Highly efficient semiconducting TiO_2 photoelectrodes prepared by aerosol pyrolysis, Electrochim. Acta 40 (1995) 643–652.
[13] Y. Lei, L.D. Zhang, J.C. Fan, Fabrication, characterization and Raman study of TiO_2 nanowire arrays prepared by anodic oxidative hydrolysis of $TiCl_3$, Chem. Phys. Lett. 338 (2001) 231–236.
[14] W. Que, A. Uddin, X. Hu, Thin film TiO_2 electrodes derived by sol–gel process for photovoltaic applications, J. Power Sources 159 (2006) 353–356.
[15] L. Sun, P. Hou, Spectroscopic ellipsometry study on e-beam deposited titanium dioxide films, Thin Solid Films 455–456 (2004) 525–529.
[16] S.F. Wang, Y.F. Hsu, Y.S. Lee, Microstructural evolution and optical properties of doped TiO_2 films prepared by RF magnetron sputtering, Ceram. Int. 32 (2006) 121–125.
[17] X. He, X. Zhao, B. Liu, Studies on a possible growth mechanism of silver nanoparticles loaded on TiO_2 thin films by photoinduced deposition method, J. Non-Cryst. Solids 354 (2008) 1267–1271.
[18] F. Meng, Z. Sun, Enhanced photocatalytic activity of silver nanoparticles modified TiO_2 thin films prepared by RF magnetron sputtering, Mater. Chem. Phys. 118 (2009) 349–353.
[19] W.T. Lim, C.H. Lee, Highly oriented ZnO thin films deposited on Ru/Si substrates, Thin Solid Films 353 (1999) 12–15.
[20] M.J. Soileau, W.E. Williams, N. Mansour, E.W. Van Stryland, Laser-induced damage and the role of self-focusing, Opt. Eng. 28 (1989) 1133–1144.
[21] E.W. Van Stryland, Y.Y. Wu, D.J. Hagan, M.J. Soileau, K. Mansour, Optical limiting with semiconductors, J. Opt. Soc. Am. B 5 (1988) 1980–1988.
[22] M.J. Soileau, W.E. Williams, E.W. Van Stryland, Optical power limiter with picosecond response time, IEEE J. Q. Elect. QE-19 (1983) 731–735.
[23] K. Mansour, M.J. Soileau, E.W. Van Stryland, Nonlinear optical properties of carbon-black suspensions (ink), J. Opt. Soc. Am. B 3 (1992) 1100–1109.
[24] M. Radecka, TiO_2 for photoelectrolytic decomposition of water, Thin Solid Films 451–452 (2004) 98–104.
[25] K. Zakrzewska, Titanium Dioxide Thin Films for Gas Sensors and Photonic Applications, vol. 155, Wydawnictwa AGH, Kraków, 2003, p. 1.
[26] K. Koski, J. Hölsä, P. Juliet, Properties of aluminium oxide thin films deposited by reactive magnetron sputtering, Thin Solid Films 339 (1999) 240–248.
[27] N. Serpone, D. Lawless, R. Khairutdinov, Subnanosecond relaxation dynamics in TiO_2 colloidal sols (particle sizes Rp = 1.0–13.4 nm). Relevance to heterogeneous photocatalysis, J. Phys. Chem. 99 (1995) 16655–16661.
[28] D. Di Claudio, A.R. Phani, S. Santucci, Enhanced optical properties of sol–gel derived TiO_2 films using microwave irradiation, Opt. Mater. 30 (2007) 279–284.
[29] B.E. Sernelius, K.F. Berggren, Z.C. Jin, I. Hamberg, C.G. Granqvist, Band-gap tailoring of ZnO by means of heavy Al doping, Phys. Rev. B 37 (1988) 10244–10248.
[30] E. Mollwo, in: R.G. Breckenridge, B.R. Russell, E.E. Hahn (Eds.), Proc. Photoconductivity Conf., Wiley, New York, 1954, p. 509.
[31] J. Yu, X. Zhao, Q. Zhao, Effect of surface structure on photocatalytic activity of TiO_2 thin films prepared by sol–gel method, Thin Solid Films 379 (2000) 7–14.
[32] G.H. Li, L. Yang, Y.X. Jin, L.D. Zhang, Structural and optical properties of TiO_2 thin film and TiO_2 + 2 wt.% $ZnFe_2O_4$ composite film prepared by r.f. sputtering, Thin Solid Films 368 (2000) 164–167.
[33] S.S. Lin, S.C. Chen, Y.H. Hung, TiO_2 nanoceramic films prepared by ion beam assisted evaporation for optical application, Ceram. Int. 35 (2009) 1581–1586.
[34] T. Yamamoto, T. Shiosaki, A. Kawabata, Characterization of ZnO piezoelectric films prepared by rf planar-magnetron sputtering, J. Appl. Phys. 51 (6) (1980) 3113–3120.
[35] D.V. Morgan, Y.H. Aliyu, R.W. Bunce, A. Salehi, Annealing effects on opto-electronic properties of sputtered and thermally evaporated indium-tin-oxide films, Thin Solid Films 312 (1998) 268–272.
[36] J.F. Nye, Physical Properties of Crystals: Their Representation by Tensors and Matrices, Oxford Science, New York, 1992.
[37] W. Lukosz, P. Pliska, Determination of thickness, refractive indices, optical anisotropy of, and stresses in SiO_2 films on silicon wafers, Opt. Commun. 117 (1995) 1–7.
[38] G.S. Vicente, A. Morales, M.T. Gutierrez, Preparation and characterization of sol–gel TiO_2 antireflective coatings for silicon, Thin Solid Films 391 (2001) 133–137.
[39] S.S. Lin, D.K. Wu, Enhanced optical properties of TiO_2 nanoceramic films by oxygen atmosphere, J. Nanosci. Nanotechnol. 10 (2010) 1099–1104.
[40] B. Hunsche, M. Vergöhl, H. Neuhäuser, F. Klose, B. Szyszka, T. Matthée, Effect of deposition parameters on optical and mechanical properties of MF- and DC-sputtered Nb_2O_5 films, Thin Solid Films 392 (2001) 184–190.